

## **Drag-Free Performance of the ST7 Disturbance Reduction System Flight Experiment on the LISA Pathfinder**

**Peiman G. Maghami<sup>(1)</sup>, James R. O'Donnell, Jr.<sup>(1)</sup>, Oscar H. Hsu<sup>(1)</sup>, John K. Zeimer<sup>(2)</sup>,  
Charles E. Dunn<sup>(2)</sup>**

*<sup>(1)</sup> Attitude Control Systems Engineering Branch, NASA Goddard Space Flight Center, Greenbelt,  
MD 20771 USA. +1 301-286-6615, Peiman.maghami@nasa.gov*

*<sup>(2)</sup> Jet Propulsion Lab, Pasadena, CA 91109, USA*

### **ABSTRACT**

The Space Technology-7 Disturbance Reduction System (DRS) is an experiment package aboard the European Space Agency (ESA) LISA Pathfinder spacecraft. LISA Pathfinder launched from Kourou, French Guiana on December 3, 2015. The DRS is tasked to validate two specific technologies: colloidal micro-Newton thrusters (CMNT) to provide low-noise control capability of the spacecraft, and drag-free control/flight. This validation is performed using highly sensitive drag-free sensors, which are provided by the LISA Technology Package of the European Space Agency. The Disturbance Reduction System is required to maintain the spacecraft's position with respect to a free-floating test mass to better than  $10\text{nm}/\sqrt{\text{Hz}}$ , along its sensitive axis (axis in optical metrology). It also has a goal of limiting the residual accelerations of any of the two test masses to below  $3 \times 10^{-14} (1 + [f/3 \text{ mHz}]^2) \text{ m/s}^2/\sqrt{\text{Hz}}$ , over the frequency range of 1 to 30 mHz.

This paper briefly describes the design and the expected on-orbit performance of the control system for the two modes wherein the drag-free performance requirements are verified. The on-orbit performance of these modes are then compared to the requirements, as well as to the expected performance, and discussed.

### **1 INTRODUCTION**

The DRS is an experiment package aboard the European Space Agency (ESA) LISA Pathfinder spacecraft. LISA Pathfinder (LPF) launched from Kourou, French Guiana on December 3, 2015. The DRS is a project managed by the NASA Jet Propulsion Laboratory, and is tasked to validate two specific technologies: colloidal micro-Newton thrusters (CMNT) to provide low-noise control capability of the spacecraft, and drag-free control/flight [1]. The CMNT systems was developed by Busek Inc., and the Dynamic Control System (DCS) algorithms and flight software for drag-free control were developed at the NASA Goddard Space Flight Center. The DRS uses highly sensitive drag-free sensors (DFS), which are provided by the LISA Technology Package (LTP) [2], of the European Space Agency, to validate its technologies.

The DRS started its operations on August 14, 2016, after three periods of commissioning. All control modes and mode transitions were successfully tested and validated during commissioning [3]. The DRS is required to demonstrate the capability of maintaining the spacecraft's position with respect to a single free-floating test mass to better than  $10\text{nm}/\sqrt{\text{Hz}}$ , along the sensitive axis (axis

connecting two test masses), over the frequency range of 1 to 30 mHz. This requirement is verified in the Drag-Free Low Force mode (DFLF). It also has a requirement of maintaining the spacecraft's position with respect to two free-floating test masses to better than  $10\text{nm}/\sqrt{\text{Hz}}$ , along the sensitive axis with a goal of limiting the residual accelerations of those test masses to below  $3 \times 10^{-14} (1 + [f/3 \text{ mHz}]^2) \text{ m/s}^2/\sqrt{\text{Hz}}$ , over the frequency range of 1 to 30 mHz. These requirements were evaluated and verified in the Science mode (18-DOF) of the mission. This paper briefly describes the design and expected performance (based on high fidelity simulation models) of the control system for the DFLF and 18-DOF modes. The control system used two clusters of four micro-Newton thrusters for spacecraft attitude and position control, along with electrostatic actuation capability of the test masses, provided by the LTP. The sensing signals for the control loops were provided by the capacitive sensing of the LTP, with the option of using the Optical Measurement System (OMS) in six degrees of freedom for significantly better accuracy and resolution. Both capacitive-only sensing as well as capacitive-and-optical sensing options were exercised in flight. However, the drag-free and acceleration requirements were verified using the flight OMS data. The OMS flight data from multi-day noise runs, along with coherent electrostatic actuation commands, were used to construct spectra of the test mass position errors, as well as test mass residual accelerations. These were compared to the requirements, as well as to the predicted spectra from simulation models. This paper provides an assessment and discussion of the drag-free performance.

## 2 ST7-DRS OVERVIEW

NASA's contribution to the LPF was the DRS experiment. The DRS consists of the Integrated Avionics Unit (IAU) and two clusters of CMNTs. The IAU performed two major software functions: Command and Data Handling (C&DH) and the DCS. The C&DH was responsible for DRS Mission Mode configuration by commanding the DCS into the correct control modes (spacecraft, Reference Test Mass (RTM), and Non-Reference Test Mass (NTM)), commanding the LTP inertial sensors into the correct sensing/actuation modes, as well as issuing commands to the CMNTs. The DRS Mission Modes are shown in Figure 1.

There are six DRS Mission Modes managed by the IAU: Standby, Attitude Control, Zero-G, Drag-Free Low Force, 18-DOF (Degree of Freedom) Transitional, and 18-DOF Mode. Standby mode is for use when the IAU is powered on but no actuation commands should be generated by the control system. Attitude Control Mode is used for the transition from LPF control to DRS Control. In this mode, the DRS nulls spacecraft attitude errors and rates while keeping the test masses centered in their housing. The Zero-G Mode is designed to use the thrusters to null out secular disturbance forces on the spacecraft, such as those from solar radiation pressure, to reduce the electrostatic forces being applied to the reference test mass. The Drag Free Low Force (DFLF) Mode is the first time the spacecraft position is controlled via thrusters to follow the reference test mass in all translational axes. Hence, it is the first mode wherein drag-free flight of a single test mass is achieved. Note that there are no electrostatic forces being commanded on the reference test mass and the reference test mass is in its high resolution capacitive measurement mode. 18-DOF Transitional is a transitional mode to get to 18-DOF control of the spacecraft and two test masses. Each of these DRS Mission Modes consists of a spacecraft control mode, a test mass control mode for each test mass, and a test mass force mode. The details of the spacecraft and test mass control design for each mode may be found in [4]-[7].

DRS Mission Mode	Spacecraft Control Mode	Reference Test Mass Control Mode	Reference Test Mass Force Mode	Non-Reference Test Mass Control Mode	Non-Reference Test Mass Force Mode
Standby	Standby	DFS Standby	N/A	DFS Standby	N/A
Attitude Control	Attitude-Only	DFS Accelerometer	High Force	DFS Accelerometer	High Force
Zero-G	Accelerometer				
Drag Free Low Force	Drag Free 1	DFS Drag Free 1	Low Force	Suspended Drag Free 1	Low Force
18-DOF Transitional					
18-DOF	Science	DFS Drag Free 2		Suspended Drag Free 2	

**Figure 1 Dynamic Control System Mode Transition Diagram**

### 3 REQUIREMENTS

The top-level requirements are mainly on the drag-free performance and the spacecraft ACS. However, there are also goals on the desired residual accelerations on the test masses, which are flowed down as requirements to the DCS. These requirements and goals are discussed in the next sections.

#### 3.1 Drag-Free Requirements

The drag-free requirement in the DFLF mode is applicable to the RTM in the sensitive axis. This requirement is summarized as follows.

*The DRS shall maintain the spacecraft position with respect to the reference test mass, about the sensitive axis (X-axis of the LTP housing frames H1 or H2), to better than  $10 \text{ nm}/\sqrt{\text{Hz}}$  in the measurement bandwidth (MBW).*

This requirement is verified in the DFLF. However, a similar requirement is also imposed in the 18-DOF mode.

#### 3.2 Acceleration Goal

There are no requirements on the test mass residual accelerations. However, there is a stated goal.

*DRS control shall strive to meet the goal of maintaining the residual accelerations along the measurement axes of both test masses to better than  $30(1+f/(3 \text{ mHz})^2) \text{ fm/s}^2 / \sqrt{\text{Hz}}$  in the*

*measurement band.*

The reason this is a goal, and not an explicit requirement, is that meeting it would depend on the performance of the LTP sensor, which is not part of the DRS experiment. In order to meet the goal of reducing residual acceleration levels of the test mass in the sensitive axis, the following requirements are imposed on the position and attitude errors of both test masses.

*The DCS shall maintain the spacecraft position with respect to the test masses, about the sensitive axis (X-axis of the LTP housing frames H1 or H2), to better than  $10 \text{ nm}/\sqrt{\text{Hz}}$  in the measurement bandwidth (MBW). The measurement bandwidth covers the frequency range of 1 mHz to 30 mHz.*

*The DCS shall maintain the spacecraft position with respect to the either test mass, about the H1Y (or H2Y), to better than  $30(1+f/(3 \text{ mHz})^2) \text{ nm}/\sqrt{\text{Hz}}$  in the MBW.*

*The DCS shall maintain the spacecraft position with respect to the either test mass, about the H1Z (or H2Z), to better than  $60(1+f/(3 \text{ mHz})^2) \text{ nm}/\sqrt{\text{Hz}}$  in the MBW.*

*The DCS shall maintain the relative attitude of the either test mass with respect to its housing, about any axis, to better than  $500(1+f/(3 \text{ mHz})^2) \text{ nrad}/\sqrt{\text{Hz}}$  in the MBW.*

## 4 18-DOF CONTROL DESIGN

In the 18-DOF mode, the spacecraft translation is controlled by the DRS control to follow one of the test masses (RTM) in three translational axes, thereby providing for drag-free flight of the RTM. The position of the NTM with respect to the spacecraft is controlled via electrostatic test mass control in all translational axes. The bandwidths of the controllers were chosen well below the MBW, particularly for controls along the sensitive axis, to meet the drag-free requirements. This was also challenging given the destabilizing effects of differential stiffness on the NTM. Differential stiffness refers to the difference of total stiffness (electrostatic and gravitational) between the NTM and the RTM. The spacecraft attitude is controlled in low frequencies (well below MBW) to maintain pointing with respect to the LPF-provided target quaternion. The target quaternion ensures constant sun pointing attitude, as well as continuity in the line of sight to the ground stations. Given the freedom at or above MBW, the spacecraft torque control is used to follow (in the MBW): (a) the non-reference test mass (NTM) in the transverse directions (normal to the LTP axis); and (b) the attitude of the RTM about the sensitive axis. This is implemented via a controller referred to as the Complementary Attitude Controller (CAC). Finally, the attitude of both test masses is controlled via electrostatic suspension well below the MBW to meet the above requirements. Details of design and analysis of all controllers in 18-DOF may be found in [7]. All controllers in 18-DOF, with one exception, are designed using single degree of freedom classical techniques, with or without torque/force feedforwarding. The design of the only exception, the CAC, is summarized in the next section.

#### 4.1 Complementary Attitude Controller

The architecture of the CAC is shown in Figure 2. The differential position error of the test masses in the transverse direction is used to compute the attitude error (in DFS frame) of the spacecraft about the RTM along the transverse axes (y and z). The roll attitude error of the RTM is used as the spacecraft attitude error along the roll of the DFS frame. The required rotation command is then transformed into the body frame and is used as an input to a SISO-based controller to control the spacecraft attitude in the measurement band, with the aid of a high-pass filter. To obtain a pure rotation about the RTM, feed-forward translation commands are generated and issued to the drag-free controller.

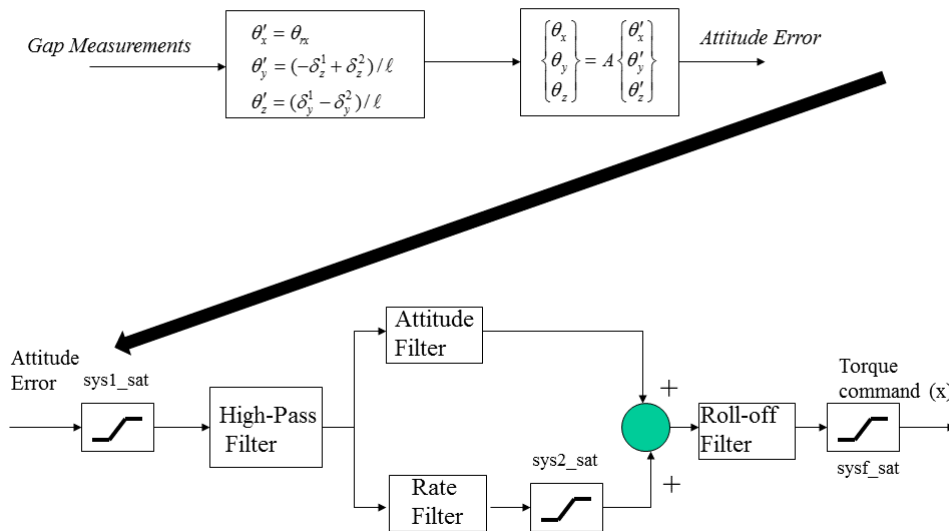


Figure 2 Complementary Attitude Controller

## 5 PERFORMANCE SUMMARY

The DRS started its nominal mission on August 14, 2016 (DOY 227). A typical time history of the spacecraft attitude error, along with the DCS commanded forces and torques, from Lisa Pathfinder handover to DRS' science mode (18-DOF) are shown in Figure 3. Corresponding test mass position and attitude errors are shown in Figures 4 and 5. The spacecraft attitude errors and the test mass position and attitude errors are well within the expected performance range. The spacecraft force and torque commands, CMNT commands, and the test electrostatic force and torque commands are



well within their expected range. This data is from the DOY 276-277. The DCS has been performing well, without any issues, since commissioning. The DCS requirements for its initial modes are mainly to maintain the spacecraft attitude, to operate the test masses as accelerometers (to support colloidal thruster experiments), and to offset the secular forces on the spacecraft. The performance requirements in the DCS's higher mode are mainly on the drag-free performance (to support science noise measurements, as well as thruster experiments) and the spacecraft ACS.

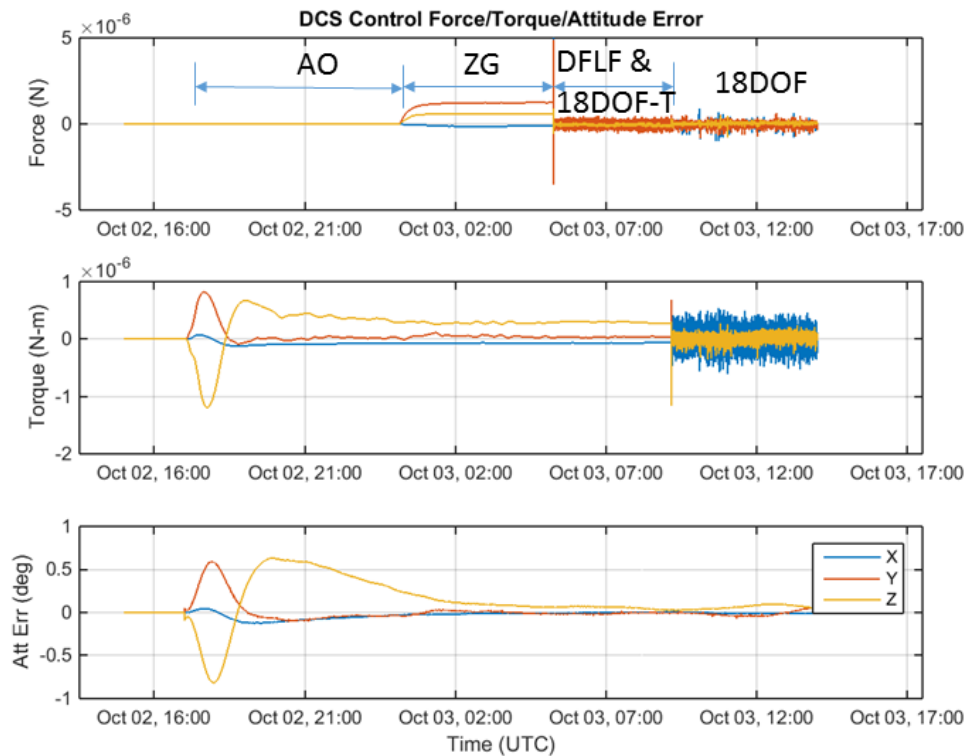


**Figure 3 Time Histories of Spacecraft Force and Torque Commands, and Attitude Errors**

The DRS baseline architecture was based on capacitive sensing only measurements for test mass position and attitude control. However, this implementation was only used during the first week of operations. Because of substantially superior noise performance of the OMS, and noise and non-stationary issues of capacitive sensing, the decision was made to switch to a mixed capacitive/optical sensing. The OMS signals can only provide interferometric measurements for the RTM X-position error, the RTM Y and Z attitude errors, the differential RTM/NTM X-position error, and the NTM Y and Z attitude errors. Therefore, the remaining degrees of freedom must continue to be measured via capacitive sensing. Additionally, the reference of the measurement error for the x-position control of the NTM was changed from the housing to the RTM, i.e., the OMS' differential X-position signal was used directly in the control loop for NTM's X-axis position control. This change was motivated to reduce the impact of spacecraft noise sources (including thruster noise) on the NTM, as well as the differential signal. The measurement signal map in the mixed measurement mode was as follows, where CAP denotes capacitive sensing.

	<b>X- Axis</b>	<b>Y- Axis</b>	<b>Z- Axis</b>
<b>RTM Position</b>	OMS 1x	CAP 1y	CAP 1z
<b>RTM Attitude</b>	CAP 1roll	OMS 1tip	OMS 1tilt
<b>NTM Position</b>	OMS2x-OMS1x	CAP 2y	CAP 2z
<b>NTM Attitude</b>	CAP 2roll	OMS 2tip	OMS 2tilt

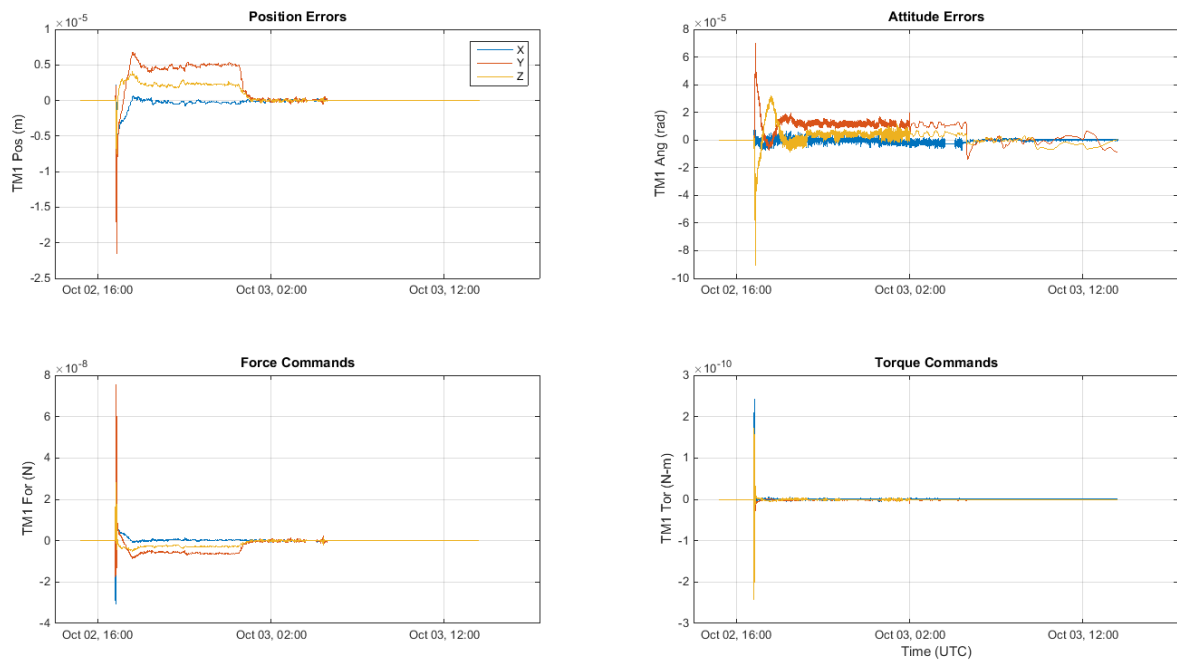


**Figure 4 Time Histories of Position/Attitude Errors and Force/Torque Commands for the RTM**

The position accuracy performance of the DRS in DFLF is discussed in section 5.1. The test mass acceleration requirements, in terms of flowed-down drag-free requirements on the test mass degrees of freedom, are discussed in section 5.2. Finally, the explicit acceleration requirements are discussed in terms of differential test mass accelerations in section 5.3.

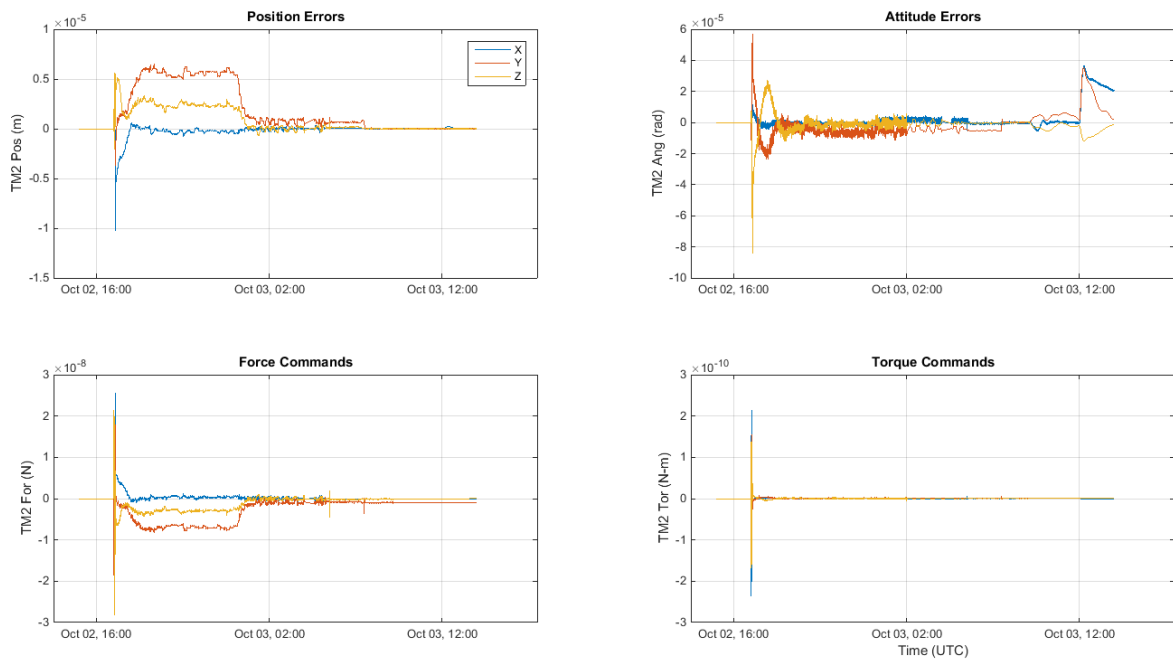


**Figure 5 Time Histories of Position/Attitude Errors and Force/Torque Commands for the NTM**

## 5.1 POSITION ACCURACY

The spacecraft position accuracy requirement (Drag-Free) requirement was verified in the DFLF mode of the DRS. This mode is the first mode in which thruster-based spacecraft control is used to establish drag-free motion of one of the test masses. A typical performance is shown in Figure 6, based on the OMS flight data (provided at 10Hz) from the DOY 235 (corresponding to August 22, 2016), while the DRS was operating in the DFLF mode, with test mass 1 as the reference test mass. Figure 6 shows the time history of the test mass position error measurements (from the OMS) for the period from DOY 235 (11:53 UTC) to DOY 236 (11:54 UTC). The DRS was in the DFLF during the first ~16.5 hours of this period.

The requirement in position accuracy is verified by comparing the amplitude spectral density of test mass position error against the DRS requirement within the band of 1 to 30 mHz. The amplitude spectral density of the measured flight data along with the DRS requirement are illustrated in Figure 7. The spectral density was generated from the first 16 hours of test mass position error data (see Figure 6). The DRS clearly meets its requirement within the 10 nm/ $\sqrt{\text{Hz}}$  required band, with significant margin. In fact, the requirement level is met at all frequencies. The noise floor, which typically is dominated by the test mass position sensing noise at the higher end of the band, was at or around 2nm. This is likely due to suppressed thrust noise, as the OMS noise is well below 2nm. The narrow band spike at around 6mHz, peaking at ~5nm, is likely attributed to the LTP hardware electronics, or other spacecraft processes, e.g., the Cold Gas thermal control system, as it is not observed in the differential signal (position of test mass 2 relative to test mass 1), or in the colloidal noise dynamics.



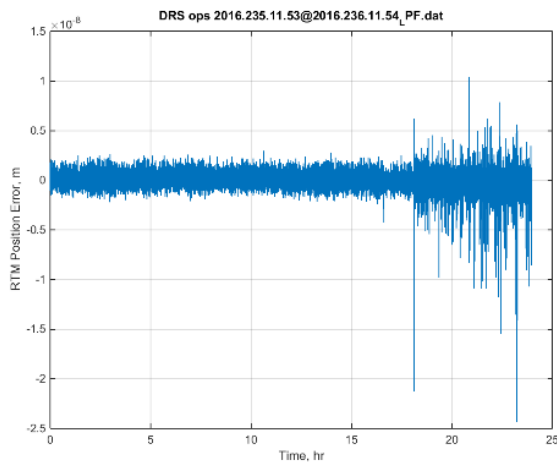


**Figure 6 Time History of Position Error Measurements for Test Mass 1**

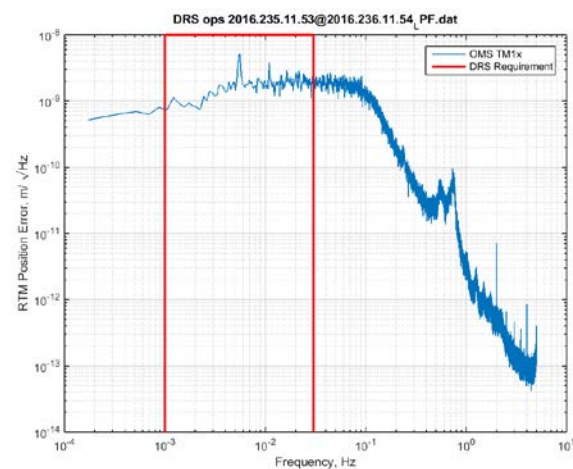


**Figure 7 Amplitude Spectral Density of Position Error for Test Mass 1**

## 5.2 TEST MASS ACCELERATIONS: DRAG-FREE REQUIREMENTS

As indicated earlier, the acceleration noise is a DRS goal, which was flowed down to the DCS in the form of drag-free requirements on the test mass position and attitude accuracy in the MBW. These requirements are verified by comparing the amplitude spectral density of test mass position/attitude errors against their corresponding limits within the band of 1 to 30 mHz. The amplitude spectral density of the flight test mass data, along with the DCS requirement, are illustrated in Figure 7. The spectral densities were generated from the flight data on DOY 257 (14:12 UTC) to DOY 258 (07:45 UTC). The data is from the OMS measurements of the RTM 1 position with respect to its housing, and the differential position of the test masses. The DCS clearly meets its requirement of 10 nm/ $\sqrt{\text{Hz}}$  for both test masses, within the required band, and with significant margin. In fact, the requirement level is met at almost all frequencies. It should be pointed out that the electrostatic actuation authority in week 5 (which includes DOY 257-258), and following noise runs in 18-DOF, were conservatively reduced in all test mass degrees of freedom in order to reduce the electrostatic suspension noise. This was of particular impact for the electrostatic force limits, along the X-axis, and torque limits, along the Z-axis, as these degrees of freedom are coupled through the electrodes they share for actuation. This mode of operation is referred to as the DRS Ultra-Ridiculously Low Authority (DURLA). The DURLA actuation limits for both test masses are shown in table 1.

**Table 1 Nominal and DURLA Actuation Limits (Forces in pN, and Torques in pNm)**

DOF	X1-Force	Y1-Force	Z1-Force	X1-Torque	Y1-Torque	Z1-Torque
<b>Nominal</b>	0	0	0	16.4	13.3	10.4
<b>DURLA</b>	0	0	0	4	4	1.5
DOF	X2-Force	Y2-Force	Z2-Force	X2-Torque	Y2-Torque	Z2-Torque
<b>Nominal</b>	2200	3670	5826	16.4	13.3	10.4
<b>DURLA</b>	100	2000	500	4	4	1

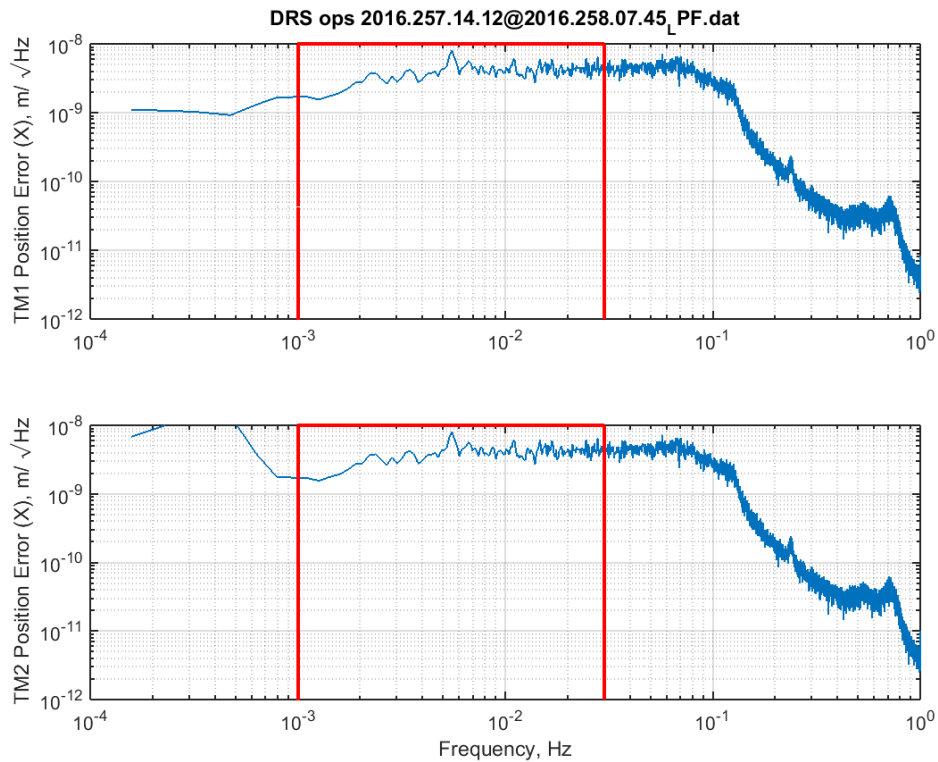


**Figure 8 Amplitude Spectral Densities of the Test Mass Position Errors along the Sensitive Axis (X)**

The requirements on position errors along the lateral axis were similarly verified, except with capacitive sensing flight data from the Inertial Sensor. The amplitude spectra for the lateral axis are shown in Figures 8 and 9. The DCS requirements are clearly met, with substantial margins. Although not shown here, the same holds true for the requirements for test mass attitudes. In fact, the Dynamic Control System met all its requirements, with considerable margin. The noise performance, in general, is better than expected mainly due to the LTP hardware and the micro-Newton thrusters performing better than their specifications.

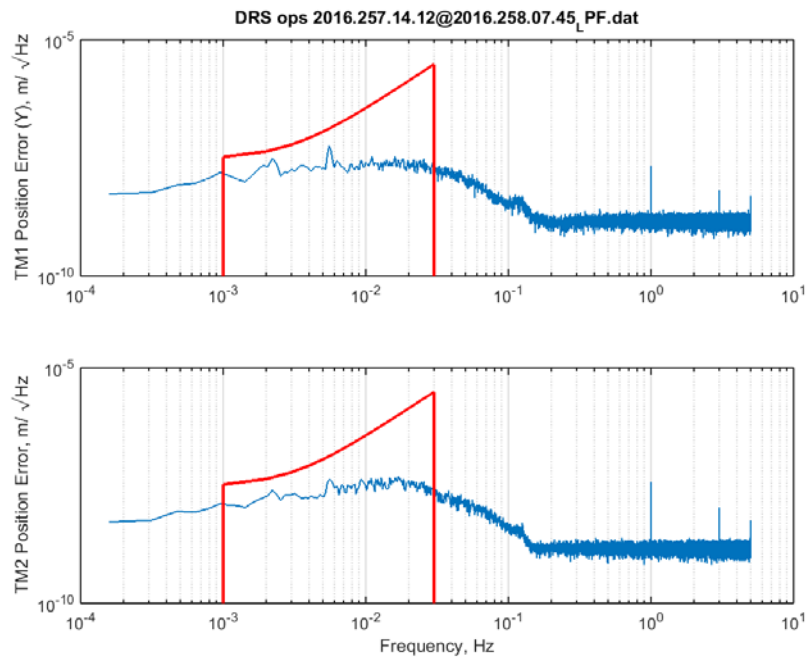


**Figure 9 Amplitude Spectral Densities of the Test Mass Position Errors along Y-axis**

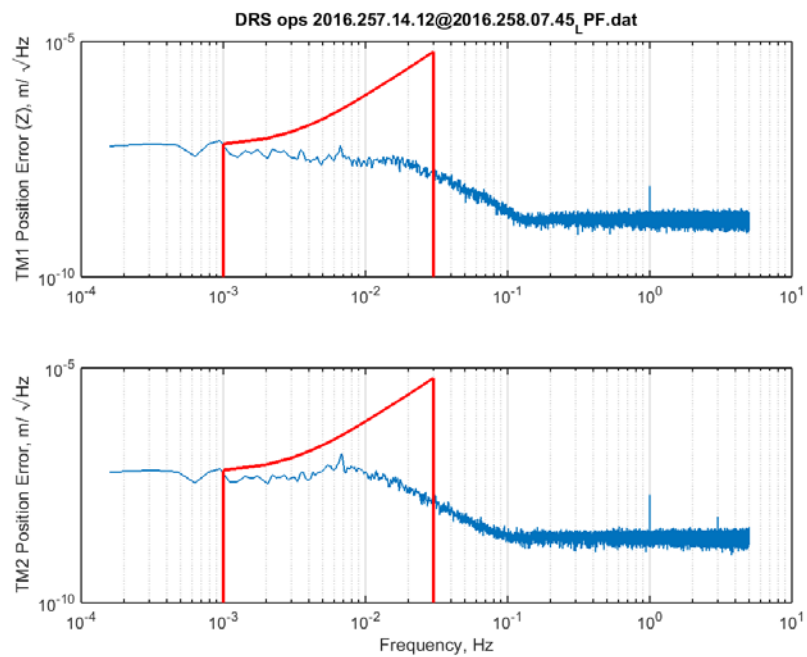


**Figure 10 Amplitude Spectral Densities of the Test Mass Position Errors along Z-axis**

### 5.3 DIFFERENTIAL ACCELERATION

Given that the DCS met all its drag-free flowed down requirements with considerable margin, it

was expected that the residual noise goal for the test masses (*to better than  $30(1+f/(3 \text{ mHz})^2) \text{ fm/s}^2/\sqrt{\text{Hz}}$  in the measurement band*) would be easily met as well. There are no direct measurements of test mass accelerations in the OMS or capacitive sensing data. Direct double differentiation of test mass positions (with respect to their housings) was hampered by the spacecraft noise (due to thrusters and others). Furthermore, capacitive sensing data was too noisy for double differentiation. However, the double time derivative of the OMS differential signal (which measures the relative position of test mass 2 to 1) along the X-axis, scaled by  $1/\sqrt{2}$ , provided a reasonable estimate of the average test mass acceleration. This is based on an assumption that the acceleration noise of the test masses is effectively uncorrelated within the MBW. Another way of stating this is that the differential test mass acceleration must be no greater than  $\sqrt{2} 30(1+f/(3 \text{ mHz})^2) \text{ fm/s}^2/\sqrt{\text{Hz}}$ . The differential acceleration performance is provided in Figure 11. In this figure, four acceleration plots are provided, one for week 1 (with capacitive sensing only in the loop), one from week 2 (with mixed capacitive/OMS sensing), one for week 5 (with DURLA activation), and finally one from the high-fidelity model (HiFi) predict. This model includes a high-fidelity model of the LPF and the LTP, provided by ESA, which is then merged with a high-fidelity model of the DRS control system and the CMNT. The differential acceleration plots have been corrected by taking out the contribution of the known acceleration commands for the RTM.

It is clear from Figure 11 that differential noise levels meet the requirement, with substantial margin. There is a slight noncompliance of the predicted acceleration at  $\sim 1 \text{ mHz}$  compared to three on-orbit acceleration curves. It is not fully clear what is driving the noncompliance. However, it may be related to larger than specified direct acceleration noise on the test masses, orbital models impacting centrifugal accelerations, or differential stiffness. As expected, the mixed capacitive/OMS sensing provided an improved performance over capacitive-only sensing, particularly in the mid-MBW, due to improved sensing noise and cross-talk. The reduced suspension noise due to DURLA provided significant further improvement in the low to mid frequencies. Unfortunately, an experiment planned for Week 12 using further reductions to the DURLA limits was not performed due to a failure of one CMNT.

The differential acceleration noise, with and without correction for the NTM electrostatic actuation force command, along the X-axis (F2X), are provided in Figures 12 and 13 for the capacitive sensing and OMS, respectively. Clearly, there are contributions from the spacecraft motion, capacitive sensing noise, and sensing/actuation cross-talk bleeding into the X-axis actuation force command of the NTM, as observed in Figure 12. As mentioned earlier, the NTM was initially controlled relative to its housing during week 1 (Capacitive sensing). However, with the adaptation of mixed sensing, the NTM was then controlled relative to the RTM from second week on, hence reducing the impact of the spacecraft motion on the control of the NTM. The X-axis position control loop of the NTM was designed to have a very low bandwidth, with the crossover frequency at  $\sim 0.28 \text{ mHz}$ , thus limiting direct electrostatic acceleration in the MBW. This is clearly evident in Figure 13, wherein little difference between the corrected and uncorrected differential noise is seen in the measurement band.

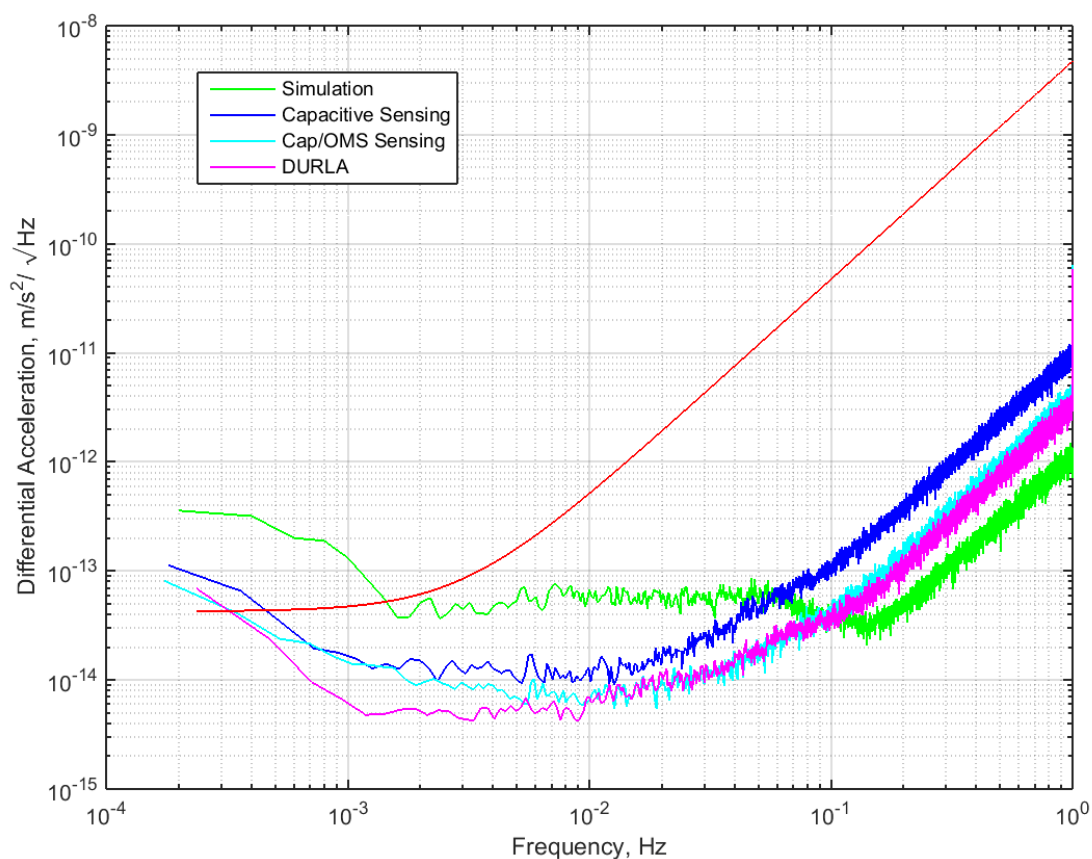


**Figure 11 Corrected Differential Acceleration Noise Performance**

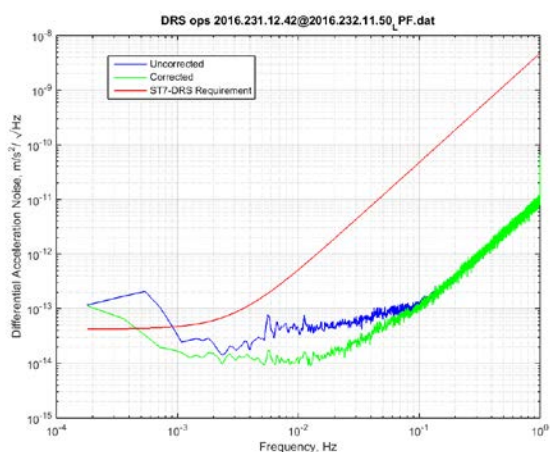


**Figure 12 Differential Acceleration Noise,  
Capacitive Sensing**

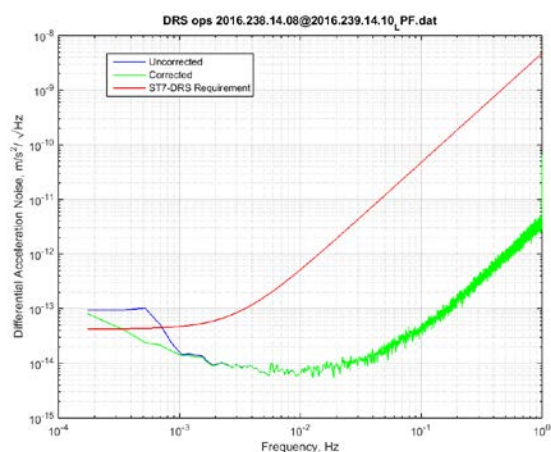


**Figure 13 Differential Acceleration Noise,  
Capacitive and OMS Sensing**



## 6 SUMMARY

The Disturbance Reduction System and the Dynamic Control System have met all their position accuracy and drag-free requirements, as well as the goal on test mass residual accelerations within the MBW, with significant margins. The noise performance, in general, was substantially better than expected mainly due to the LTP and the micro-Newton thrusters performing better than their requirements. All control modes performed nominally, with good robustness characteristics. The mixed capacitive/optical sensing was adopted early in the mission operations to take advantage of the stability and noise performance of the optical sensing in the drag-free and noise runs. Finally, the noise performance was further enhanced by reducing the electrostatic actuation authority.

## 7 ACKNOWLEDGEMENTS

The authors would like to acknowledge the hard work and dedication of many individuals without whom this mission would not have been possible. Some of these include Jeff D'Agostino and Kathie Blackman of the Hammers Co., who implemented the DCS algorithms into flight software and tested them, as well as supplying simulators to JPL and ESA. Phil Barela, Bill Folkner, Andrew Romero-Wolf, and Mike Girard were just a few of the many engineers at JPL who helped make the mission a success. The DRS mission would not have been possible without the CMNTs developed by Vlad Hruby and the Busek Co. We also received invaluable assistance with our experiment from engineers at Airbus Defence and Space in Stevenage, UK, and from mission operations personnel at the European Space Operations Centre (ESOC) in Darmstadt, Germany, as we readied our experiment for launch and then throughout commissioning and operations. In particular, we would like to express our gratitude to Jose Mendes and Ian Harrison of ESOC for their continued support and invaluable insights. Finally, we'd like to thank all of the members of the LISA Pathfinder spacecraft and science teams, especially Project Scientists Paul McNamara and Martin Hewitson and Goddard scientists Ira Thorpe and Jake Slutsky.

## 8 REFERENCES

1. Carmain, A., et. al., "Space Technology 7 Disturbance Reduction System—Precision Control Flight Validation," IEEE Aerospace Conference, Big Sky, MT, USA, March 2005.
2. McNamara, P., et. al., "LISA Pathfinder," Classical Quantum Gravity, 25, 114034 (2008).
3. Hsu, O. C., et. al., "Dynamic Control System Performance During Commissioning of the Space Technology 7 – Disturbance Reduction System Experiment on LISA Pathfinder," AAS 17-155, Proceedings of the AAS GN&C Conference, Breckenridge, CO, February 2017.
4. Maghami, P. G., et. al., "Control Modes of the ST7 Disturbance Reduction System Flight Validation Experiment," SPIE Paper 5528A-17, International Symposium on Optical Science and Technology, Denver, Colorado, USA, August 2004.
5. Hsu, O. C., et. al., "Mode Transitions for the ST7 Disturbance Reduction System



- Experiment,” AIAA Paper 2004-5429, AIAA Guidance, Navigation & Control Conference, Providence, Rhode Island, USA, August 2004.
6. O'Donnell, J. R., et. al., “The Space Technology 7 Disturbance Reduction System—Precision Control Flight Validation,” Proceedings of the 19th International Symposium on Space Flight Dynamics; 4-11 Jun. 2006; Kanazawa; Japan.
  7. Maghami, P.G., et. al., “Drag-Free Control Design for the ST7 Disturbance Reduction System Flight Experiment,” AIAA paper 2007-6733, AIAA Guidance, Navigation, and Controls Conf., Hilton Head, SC, USA, August 2007.